Ordering of conduction band states in thin-layer $(AlAs)_m(GaAs)_n(001)$ superlattices

Ordering of conduction band states in thin-layer $(AlAs)_m(GaAs)_n(001)$ superlattices

Nacir Tit†

International Centre for Theoretical Physics, Strada Costiera 11, I-34100 Trieste, Italy

Abstract. The electronic structures of thin-layer $(AlAs)_m(GaAs)_n(001)$ superlattices (SLs) are investigated versus the SL layer thicknesses (m, n) and the band offsets. The calculations are based on the empirical sp^3s^* tight-binding model, which includes only nearest-neighbour interactions. Particular attention is given to the effect of the interface parametrization on the SL electronic properties. This is done, mainly, by varying the band offsets over a sufficiently broad range. The results show that the existence of type-II behaviour in the ultrathin-layer SLs necessitates a large valence band offset (VBO $\simeq 0.56$ eV) and small conduction band offset (CBO $\simeq 190$ meV). Providing that these offset values are achieved, it is found that the highest state of the valence band is always confined to the GaAs slabs whereas the bottom state of the conduction band shows different behaviours as it is sensitive to band-mixing effects. It is due to these mixing effects that most of the ultrathin-layer SLs (with $m, n \leqslant 8$) behave as type-II heterostructures, where the electrons are localized in the AlAs X_{xy} valley. The rest of the ultrathin-layer SLs behave as type-I heterostructures with a direct bandgap at the Γ point, whenever the GaAs slabs are thick enough to make the electron confinement energy small in the GaAs wells. For thick-layer SLs, our results suggest the existence of a critical barrier thickness, beyond which the GaAs wells become completely decoupled and the SL behaves as a type I heterostructure. The estimated critical layer thickness, for the crossover from type-I to type-II behaviour, is $n_c = 9$ for the SLs with $m = n$ when using VBO $= 0.56$ eV. This n_c-value is consistent with the photoreflectance experiments. The relevance of our work to photonic device applications is discussed further.

1. Introduction

There has been great interest in short-period semiconductor superlattices (SLs) because they often possess tunable electronic properties and, hence, are suited to a variety of applications [1]. The $(AlAs)_m(GaAs)_n(001)$ superlattices, in particular, have received an enormous amount of attention as they show a variety of electronic structures depending on the choice of layer thicknesses. The top state of the valence band (VB) is always confined to the GaAs slabs whereas the bottom state of the conduction band (CB) shows different behaviours as it is sensitive to the band-mixing effects. The importance of such mixing has been demonstrated from studies of optical transition lifetimes [2, 3], from observations of ΓX anticrossing [4], from transport and electroluminescence studies [5] and from photoreflectance and photoluminescence measurements [6, 7]. Despite intensive scrutiny, the order of the low-lying conduction band valleys in these SLs remains controversial. Theoretical calculations disagree and experimentally it is difficult to disentangle intrinsic behaviour from the effects of the disorder. In spite of these difficulties, there is plentiful experimental evidence [2–7]

† Present address: Physics Department, UAE University, PO Box 17551, Al-Ain, United Arab Emirates. Fax: (03)-671-291; e-mail address: nacir@nyx.uaeu.ac.ae.

that the thin-layer SLs (with $n = m$ and smaller than a certain critical layer thickness n_c) behave as type-II heterostructures, where the electrons and holes are spatially separated—the former being localized in the AlAs slabs while the latter are confined to the GaAs layers. The disagreement arises, however, in characterizing the lowest-lying CB states of the type-II SLs in the reciprocal space. Some authors reported that these latter SLs exhibit pseudodirect transitions (i.e. the CB minimum of the SL is located at the Γ point of the SL Brillouin zone that originates from the zone-folded AlAs X_z level) whereas others reported the existence of indirect transitions (i.e. the CB minimum of the SL is located at the M point of the SL Brillouin zone that originates from the X_x and X_y levels of AlAs) and in this latter case the electrons are separated in both real and reciprocal spaces. Thus, this particular question remains open and the existing results are controversial. For instance, Fujimoto *et al* [6] carried out photoreflectance (PR) and photoluminescence (PL) measurements on short-period $(GaAs)_n(AlAs)_n(001)$ SLs, with $n = 1$–15, grown by means of molecular beam epitaxy (MBE), and their results suggest the existence of a crossover from an indirect (X_{xy}-like) to a direct transition at around $n_c = 10$. These authors, in addition, supported their experimental observations with calculations of the band structures using the sp^3s^* tight-binding model which includes the second-nearest-neighbour interactions. On the other hand, Matsuoka *et al* [7] carried out the same PR and PL measurements on MBE-grown short-period $(GaAs)_n(AlAs)_n(001)$ SLs with $n = 3$–15 and reported the existence of a crossover from a direct to a pseudodirect (X_z-like) transition at about $n_c = 12$. Moreover, these latter authors also performed energy band calculations using a (different) empirical sp^3 tight-binding model which includes the second-nearest-neighbour interactions to corroborate their experimental observations. The discrepancies between the results of reference [6] and those of reference [7] may be summarized in the two following points:

(a) From the experimental side, there is a difficulty in growing sufficiently homogeneous atomic layers and the predominant discrepancy may be attributed to the layer thickness fluctuations.
(b) On the theoretical side, however, the tight-binding parameters are affected by the interface.

Furthermore, it is obvious that the band mixing in these particular SLs is very sensitive to interface-related effects such as the atomic structure and parametrization. As far as theory is concerned, the aim of our present paper is to investigate the effects of the interface parametrization, such as band offsets, on the SL electronic properties.

It is worth noting that in the type-II SLs, the electronic transition is distinguished by the characteristics of low optical efficiency and slower photoluminescence decay rate at low temperature ($\simeq 2$ K). Thus, these SLs are believed to be of low importance as active optical materials in semiconductor devices such as light-emitting diodes. In this respect, of course, it is obvious that type-I SLs are more attractive and suitable for such applications. On the other hand, it has recently been reported [8] that at room temperature the ultrathin-layer SLs (with $m = n$) possess type-I emissions with very high external quantum efficiency. There definitely remain many open questions about the physical mechanism leading to the observed features and these are left to a forthcoming investigation.

From a theoretical point of view, the band structures of the $(AlAs)_n(GaAs)_n(001)$ SLs have been investigated by a variety of methods from the simplest Kronig–Penney (KP) calculation [9], through the Wannier-function-type calculation [10] to the sophisticated microscopic methods based on tight-binding [6–8, 11–17], empirical and self-consistent pseudopotential [18–25], or linear muffin-tin orbital (LMTO) calculations [26]. The theoretical results are contradictory and the ordering of the CB states in type-II SLs as well as the crossover from type-II to type-I behaviour are model dependent. There seems, however, to be mutual agreement

between theory and experiment [27–29] that the lowest CB state in the (AlAs)$_1$(GaAs)$_1$(001) SL is at the R point of the tetragonal Brillouin zone (t.BZ), which corresponds to the AlAs L point of the bulk Brillouin zone (b.BZ). For the ultrathin SLs with $n > 1$, however, disagreement occurs.

(a) First, the effective-mass approach (based on the Kronig–Penney model) [9] is irrelevant as it cannot take into account the band-mixing effects and, therefore, fails even to predict the existence of type-II behaviour.

(b) The Wannier-function-type calculations done by Ting and Chang [10] suggested that the X$_z$ level lies lower than the X$_{x,y}$ states. A disadvantage of the Wannier functions is the nonlocal nature (spanning 20 nearest neighbours in their case). Thus, too many Hamiltonian overlap parameters are affected by the interfaces. Such a wide interface region, obviously, greatly reduces the effective widths of the well and barrier regions. This feature makes Wannier-function calculation an inappropriate method for studying the short-period SLs. For example, the transition from type-I to type-II behaviour was found by Ting and Chang [10] to occur at about an 80 Å AlAs layer thickness as compared with the expected value of 35 Å [7, 8, 30]. The one-band Wannier function is centred on a unit cell, in contrast to the tight-binding wavefunction which is centred on an atomic site, and therefore they lead to completely different conclusions as regards the SL electronic properties.

(c) The first-principles calculations using the LDA are unable to obtain the bandgaps in the bulk correctly [31] without adjustments [19]. Even with the inclusion of these corrections, Nakayama and Kamimura [19], using a self-consistent pseudopotential method, predicted that only the (AlAs)$_1$(GaAs)$_1$ SL has an indirect bandgap at the R point of the t.BZ. A second disadvantage of the first-principles methods is their limitation to dealing with only small-size systems and, as a consequence, they are unsuitable for use in looking for the value of n_c corresponding to the crossover from type-I to type-II behaviour. They are more suited to the study of problems involving the total energy, such as that of the SL stability, rather than the conduction subbands such as is required in our present case.

For all of these reasons, we decided to adopt the sp^{3}s* tight-binding (TB) method including only the nearest-neighbour interactions [32]. To reduce the effect of the interfaces on the TB parameters, as one learned from, for instance, the Wannier-function calculations, the second-nearest-neighbour interactions are excluded. Furthermore, we prefer this scheme to the first-principles method because it is capable of reproducing more accurately the experimental bandgaps [33] as well as the respective bulk CB valleys of the GaAs and AlAs including the values of the carrier effective masses. These latter are important indicators of the accuracy of the subbands and the TB scheme thus enables us to study more broadly the dependence on layer thicknesses.

It should be noted that the disadvantage of the TB method is the lack of knowledge of the parameters across the interface. The CB states are very sensitive to both the interface parametrization and the bulk band structures of the two constituents, such as effective masses. Earlier calculations [11, 12], starting with an empirical fit to the bulk bands, took the valence band offset (VBO) to be 15% of the direct-bandgap difference between the two constituents $\Delta E_g^{(d)}$ (i.e. this choice is following Dingle's rule [34], which gives VBO $= 0.225$ eV for our present case) and yielded no type-II alignment and no valley-mixing effects. Nara [13], furthermore, took two cases of band-offset values based on Dingle's rule [34] and Kroemer's rule [35] (Kroemer's rule suggests that VBO/$\Delta E_g^{(d)} = 40\%$, which yields VBO $= 0.50$ eV for our present case) and compared the resulting band structures of ultrathin SLs to the pseudopotential calculations [19]. It was concluded from this study that Dingle's rule yields

a good description of the valence bands whereas Kroemer's rule leads to conduction bands in better agreement with the pseudopotential results. Yamaguchi [14], using the sp^3s^* TB model and Kroemer's rule for the band-offset values, has studied the band structure of the $(AlAs)_n(GaAs)_n(001)$ SLs and has shown that the lowest CB state for $n = 1$–5 is indirect and located in the X_{xy} valley and that the crossover to a direct-bandgap SL occurs at $n_c = 7$. Last but not least, two further papers [15, 16] have, specifically, addressed the valley-mixing problem for $(AlAs)_m(GaAs)_n(001)$ SLs and worked out a type-I and type-II phase diagram using the sp^3s^* TB model [32], which includes only nearest-neighbour interactions. They found that the $X_{x,y}$ levels lie lower than the X_z level in the type-II SL realizations. Ihm [15] used VBO = 0.50 eV consistently with Kroemer's rule whereas Muñoz *et al* [16] used VBO = 0.55 eV, which is in accordance with the photoluminescence data [36]. On the other hand, Lu and Sham [17] studied the electronic structures of the short-period $(AlAs)_m(GaAs)_n(001)$ SLs, with $m, n < 10$, using the sp^3 TB model including the second-nearest-neighbour interactions. Although they took VBO = 0.55 eV, like Muñoz *et al* [16] (but, of course, using a different TB model), they found a crossover from type-I to type-II behaviour, in the case of SLs with $n = m$, to occur at $n_c = 12$ and, in contrast with the results of Muñoz *et al* [16], that the X_z level lies below the $X_{x,y}$ states.

The aim of the present investigation is to shed light on the effect of the interface parametrization (and particularly the band offsets) on the $(AlAs)_m(GaAs)_n(001)$ SL band structures. Special attention will be given to the existence of type-II behaviour and the ordering of the CB states in short-period SLs when the VBO is varied over a sufficiently broad range. The method that we used in calculating the band structures is based on the sp^3s^* tight-binding model including only nearest-neighbour interactions, and will be described in some detail in the next section. Section 3 gives a discussion of our results and the final section summarizes our main conclusions.

2. Computational method

In the tight-binding framework, the Hamiltonian matrix elements are expressed in terms of a basis of symmetrically orthonormalized atomic orbitals $|b, \mu, \vec{R}_i\rangle$, also called Löwdin orbitals [37]. Here $\vec{R}_i$ denotes a Bravais lattice point referred to the unit cell, b is a basis atom in this unit cell, and μ denotes an orbital (such as s, p_x, p_y, p_z, or s*) of the atom b. In fact, in the $\vec{k}$-space, the Hamiltonian is expressed in terms of a basis $|b, \mu, \vec{k}\rangle$, which is obtained via a discrete Fourier transformation of the localized orbitals $|b, \mu, \vec{R}_i\rangle$, given by

$$|b, \mu, \vec{k}\rangle = \frac{1}{\sqrt{N_w}} \sum_j e^{i\vec{k}\cdot\vec{R}_j} |b, \mu, \vec{R}_j\rangle \tag{1}$$

where N_w is the number of $\vec{k}$-vectors taken from within the irreducible wedge of the Brillouin zone.

The Schrödinger equation whose solutions are the Bloch functions $|n\vec{k}\rangle$ is given by

$$(H - E_{n\vec{k}})|n\vec{k}\rangle = 0 \tag{2}$$

which can be expressed in terms of the Löwdin basis as

$$\sum_{j,\nu} \left[\langle i, \mu, \vec{k}|H|j, \nu, \vec{k}\rangle - E_{n\vec{k}}\delta_{i,j}\delta_{\mu,\nu} \right] \langle j, \nu, \vec{k}|n\vec{k}\rangle = 0 \tag{3}$$

where n is a band index, i and j denote basis atoms, and μ and ν denote orbitals of these respective atoms. The eigenvalues, $E_{n\vec{k}}$, and corresponding eigenvectors, $|n\vec{k}\rangle$, are obtained by means of a direct diagonalization based on the Lanczos algorithm [38] procedure. The

Table 1. Empirical sp^{3}s* tight-binding parameters for AlAs and GaAs, in units of eV. The same notation is used as in reference [32]. The bond lengths (d) are in Å.

Compound	d	$E(s, a)$	$E(p, a)$	$E(s, c)$	$E(p, c)$	$E(s^*, a)$	$E(s^*, c)$
AlAs	2.45	−7.5273	0.9833	−1.1627	3.5867	7.4833	6.7267
GaAs	2.45	−8.3431	1.0414	−2.6569	3.6686	8.5914	6.7386

Compound	$V(s, s)$	$V(x, x)$	$V(x, y)$	$V(sa, pc)$	$V(sc, pa)$	$V(s^*a, pc)$	$V(pa, s^*c)$
AlAs	−6.6642	1.8780	4.2919	5.1106	5.4965	4.5216	4.9950
GaAs	−6.4513	1.9546	5.0779	4.4800	5.7839	4.8422	4.8077

Hamiltonian, of either the bulk *fcc* structure or the *tetragonal* superlattice structure, uses the empirical tight-binding parameters given in table 1. Furthermore, one should note that in the SL electronic structure calculation one must take into account the band discontinuities [39]. In the tight-binding framework, the valence band offset is considered as a constant, and added to the diagonal elements of the Hamiltonian matrix (for instance, in our case, the GaAs on-site energies are shifted up by the VBO value because the GaAs valence band edge is higher in energy when this latter material forms an interface with the AlAs). The VBO is taken as a free parameter in our present work to assess the effect on the SL electronic properties. Moreover, the spin–orbit effects are included only in our supercell calculations, through the values used for the band offsets. Lastly, we emphasize that the on-site tight-binding parameters for the 'As' atoms across the interface are taken to be averages of the values from the two bulk regions. This choice makes the lowest CB state, in the (AlAs)$_1$(GaAs)$_1$(001) SL, located at the R point in agreement with what is well established in the literature [27–29].

In the next section, we display and discuss our results on the band structures for the (AlAs)$_m$(GaAs)$_n$(001) SLs versus the layer thicknesses (m, n) and the valence band offset (VBO).

3. Results and discussion

The bulk band-structure calculations, using the sp^{3}s* tight-binding model [32], yield a direct bandgap at the Γ point for GaAs and an indirect one at the X point for AlAs. The energy gap values obtained, neglecting spin–orbit interactions, are $E_g = 1.55$ and 2.30 eV for GaAs and AlAs respectively. Moreover, the effective masses [32] are also in good agreement with the experimental data [33].

For the band structures of (AlAs)$_m$(GaAs)$_n$(001) SLs, we start with the case of $m, n \leqslant 8$. We took in our calculation VBO = 0.56 eV unless stated otherwise in the text below. This VBO value is more reliable and consistent with experimental data [36, 40–41] and will be further commented on below. In table 2, we display the results for the bandgap energy (E_g) as well as showing the position of the bottom of the SL conduction band with respect to the high-symmetry lines in the t.BZ. As can be seen in this table, in the AlAs/GaAs thin-layer heterostructure, the potential modulation along the growth axis induces mixing of the GaAs Γ and the AlAs X electronic states and direct transitions can take place. For instance, whenever the GaAs layers are sufficiently thick, the Γ conduction subband lies below the X subband and the SL becomes of type I with a direct bandgap (see, for example, $m = 1$ with $n \geqslant 2$, $m = 2$ with $n \geqslant 6$ etc). The existence of type-I heterostructures in table 1 seems to be robust against the variation of the VBO from 0.25 to 0.56 eV, whereas for all other combinations of m and n (especially when $n \leqslant m \leqslant 8$) the SL forms a type-II heterostructure with an indirect bandgap. In the latter heterostructures, the lowest state in the SL conduction band is mainly attributed to

Table 2. The bandgap energies of the $(AlAs)_m(GaAs)_n(001)$ SLs versus m, n ($\leqslant 8$) when VBO = 0.56 eV. The position of the bottom of CB with respect to the high-symmetry lines of the t.BZ is indicated under each E_g-value. The symbol ¶ indicates the SLs of type I.

↓ $n; m \rightarrow$	1	2	3	4	5	6	7	8
1	2.12	2.11	2.15	2.17	2.18	2.19	2.19	2.20
	R	MA (80%)	MA (80%)	ΓM (90%)	ΓM (90%)	ΓM (90%)	ΓM (90%)	ΓM (90%)
2	1.98¶	2.00	2.05	2.07	2.08	2.08	2.09	2.09
	Γ	MA (80%)	MA (30%)	ΓM (90%)	ΓM (90%)	ΓM (90%)	ΓM (90%)	ΓM (90%)
3	1.86¶	1.94	1.97	1.99	2.00	2.00	2.00	2.00
	Γ	MA (30%)	M	ΓM (90%)	ΓM (90%)	ΓM (90%)	ΓM (90%)	ΓM (90%)
4	1.79¶	1.89	1.92	1.93	1.94	1.94	1.94	1.94
	Γ	M	MA (30%)	ΓM (90%)	ΓM (90%)	ΓM (90%)	ΓM (90%)	ΓM (90%)
5	1.75¶	1.86	1.88	1.89	1.89	1.89	1.89	1.89
	Γ	MA (30%)	MA (90%)	ΓM (90%)	ΓM (90%)	ΓM (90%)	ΓM (90%)	ΓM (90%)
6	1.72¶	1.82¶	1.86	1.86	1.86	1.86	1.86	1.86
	Γ	Γ	MA (90%)	ΓM (90%)	ΓM (90%)	ΓM (90%)	ΓM (90%)	ΓM (90%)
7	1.69¶	1.78¶	1.82¶	1.84	1.84	1.84	1.84	1.84
	Γ	Γ	Γ	ΓM (90%)	ΓM (90%)	ΓM (90%)	ΓM (90%)	ΓM (90%)
8	1.67¶	1.75¶	1.79¶	1.81¶	1.82	1.82	1.82	1.82
	Γ	Γ	Γ	Γ	ΓM (70%)	ΓM (90%)	ΓM (90%)	ΓM (90%)

Table 3. Same as table 2, but for the results on E_g for the $(AlAs)_n(GaAs)_n(001)$ SL versus n.

n:	1	2	3	4	5	6	7	8	9	10	15	20	25
E_g (eV):	2.12	2.00	1.97	1.93	1.89	1.86	1.84	1.82	1.80¶	1.77¶	1.68¶	1.63¶	1.61¶
	R	M	M	M	M	M	M	M	Γ	Γ	Γ	Γ	Γ

the AlAs X valley. The last remark about table 2 concerns the confinement effects. We note that for small barrier thicknesses (small m), the SL E_g decreases very rapidly toward the bulk GaAs bandgap value as n increases. On the other hand, for small well thicknesses (small n), the SL E_g increases very quickly toward the bulk AlAs bandgap value as m increases.

In figure 1, we show the band structures of the $(AlAs)_m(GaAs)_n(001)$ SLs corresponding to: (a) $m = n = 4$; (b) $m = 1$, $n = 4$; and (c) $m = n = 10$. The bandgap is indirect for figure 1(a) and direct for the other two panels and the respective energy gaps are 1.93, 1.79 and 1.77 eV. In all of these panels we have shown the four highest valence bands and the eight lowest conduction bands and taken the top of the VB as an energy reference. As can be seen in figure 1(a), the strong band mixing of electronic states, through the electronically low (and relatively short) AlAs barrier, enhances the AlAs X subband to become lower than the GaAs Γ subband. As a result, the SL becomes of type II with an indirect bandgap. On the other hand, in figure 1(b), due to the low confinement energy of the electron in the GaAs well (when this latter is much thicker than the AlAs barrier), the GaAs Γ subband is lower than the AlAs X subband and, as a consequence, the SL behaves as a type-I heterostructure. As the AlAs barrier becomes thicker than a certain critical value ($n_c = 9$ in the case of SLs with $m = n$), as shown in figure 1(c), the GaAs wells become completely decoupled and the band mixing vanishes. Hence, the electrons become localized within the GaAs Γ valley and the superlattice behaves as a type-I heterostructure with a direct bandgap at the Γ point.
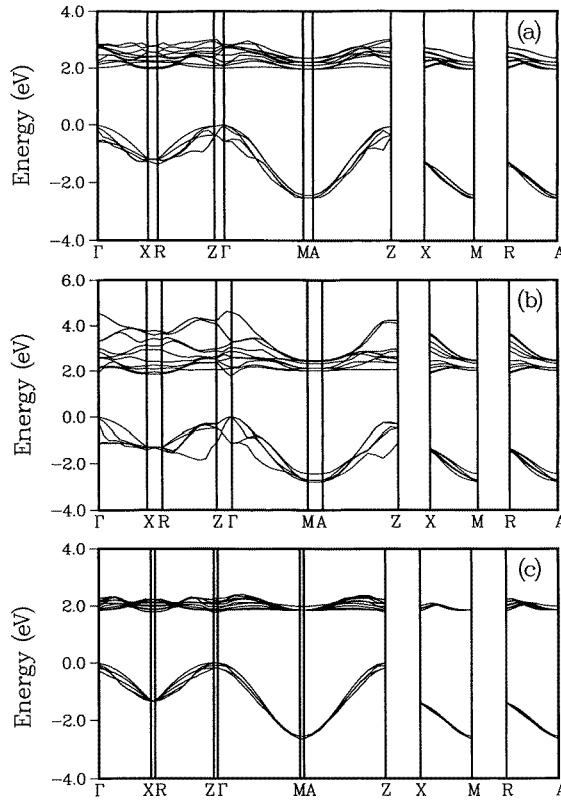
Figure 1. Band structures of the (AlAs)$_m$(GaAs)$_n$(001) superlattices with: (a) $m = n = 4$; (b) $m = 1, n = 4$; and (c) $m = n = 10$. VBO = 0.56 eV is used. The four highest valence bands and the eight lowest conduction bands are shown and the top of VB is chosen as the energy reference.

Furthermore, we have inspected the band structures of the (AlAs)$_n$(GaAs)$_n$(001) SL versus the layer thickness n ($n = 1$–25) and summarized the results in table 3 using VBO = 0.56 eV. For $n = 1$, the lowest CB state is located at the R point of the t.BZ in agreement with what is well known in the literature [27–29]. For $n = 2$–8, our results show that the lowest CB state changes its location to the M point of the t.BZ (which corresponds to the AlAs X$_{xy}$ level of the b.BZ). It is worth mentioning here that in the SL there exist two distinct X-related AlAs CB states—namely, the state with its $\vec{k}$-vector parallel to the SL growth direction, called 'X$_z$', and the one with its $\vec{k}$-vector parallel to the interface, called 'X$_{xy}$'. Within the framework of the nearest-neighbour TB approximation used here, GaAs slabs and AlAs slabs completely decouple for the X$_{xy}$ state, which is characterized as purely AlAs in its origin, whereas the X$_z$ level deviates from the bulk AlAs X level significantly due to the zone folding and the strong band mixing. For $n \geqslant 9$, the lowest CB state becomes located at the Γ point and fully localized in the GaAs slabs and, hence, the SL becomes of type I with a direct bandgap. The corresponding critical layer thickness for this type-I–type-II transition (i.e. $n_c = 9$) is therefore estimated to be about 26 Å, which is in good agreement with the photoreflectance measurements [6].

In figure 2, we show the variation of the four lowest CB states corresponding to four different high-symmetry points in the t.BZ—namely, Γ, X, R and M—versus the layer thickness
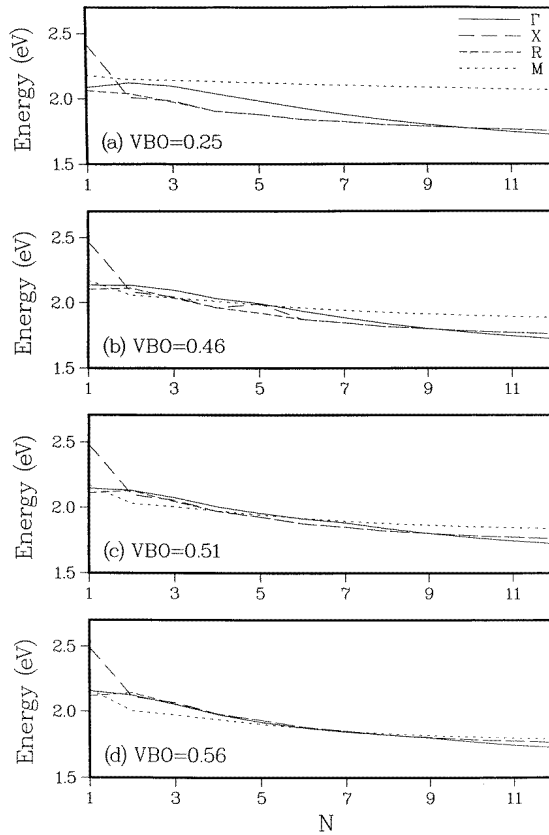
Figure 2. The ordering of the four lowest CB states corresponding to four different high-symmetry points in the t.BZ of $(AlAs)_n (GaAs)_n (001)$ SLs versus n. The VBO values used are: (a) 0.25 eV; (b) 0.46 eV; (c) 0.51 eV; and (d) 0.56 eV. The SL valence band edge is chosen as the energy reference.

n in the case of SLs with $m = n$. Different VBO values are used to assess their effects on the ordering of the CB states, especially for type-II SLs. These VBO values are taken from the literature. For instance, VBO $= 0.25$ eV was obtained by Frensley and Kroemer [42], using first-principles calculation but with respect to the average of the potentials at the two zinc-blende empty lattice sites. The second value (VBO $= 0.46$ eV) is based on the *ab initio* calculation using the Gaussian orbitals carried out by Bylander and Kleinman [23], whereas VBO $= 0.51$ eV was obtained from the *ab initio* self-consistent pseudopotential calculation of Baldereschi *et al* [43]. The last value, VBO $= 0.56$ eV, is in accordance with the photoluminescence data [36, 40–41] and lies between the two theoretical estimates of 0.51 eV (of reference [43]) and 0.60 eV of Van de Walle obtained using the model-solid theory [44]. For these different VBOs, the n_c-values obtained are $n_c = 10$ for VBO $= 0.25$, 0.46 and 0.51 eV, whereas $n_c = 9$ for VBO $= 0.56$ eV. For this latter value, the ordering of the CB states seems to be more consistent with experimental findings. In other words, for $n = 1$ we have the CB minimum at the R point, whereas for $1 < n < 9$ it is located at the M point and for $n \geqslant 9$ the SL exhibits a transition to type I. We emphasize that it is only in the case of VBO $= 0.56$ eV (figure 2(d)) that the M state does indeed correspond to the pure AlAs X_{xy} level. However, the M state in the other three panels is a mixed state and therefore

type-II behaviour occurs only when the CBO is small (such as in figure 2(d)). Thus, the value VBO = 0.56 eV seems to be the optimum for which a favourable compromise between the ordering of the CB states in type-II SLs and the value of the critical layer thickness (n_c), which is consistent with experiments [6], is achieved. This VBO value is also at 34% of the direct-bandgap difference between AlAs and GaAs, in accordance with the photoluminescence data [36, 40, 41].
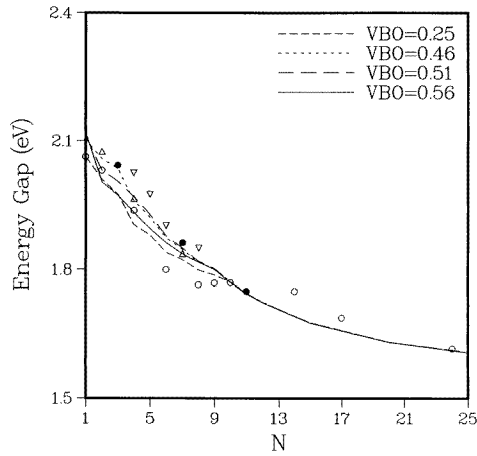
Figure 3. Comparison of the calculated energy gaps of the (AlAs)$_n$(GaAs)$_n$(001) superlattices with experiments: (O) reference [45]; (△) reference [46]; (●) reference [47]; and (∇) reference [48]. The theoretical curves correspond to four different VBO values.

Figure 3 displays the variation of the energy gap E_g versus the layer thickness n for the (AlAs)$_n$(GaAs)$_n$[001] SLs, with various VBO values. In this figure, the experimental data shown by the symbols O, △, ● and ∇ correspond respectively to the references [45], [46], [47] and [48]. As shown in this figure, the solid curve, corresponding to VBO = 0.56 eV, lies in between the other three theoretical curves and also is the least-squares fit to the scattered experimental data. Our theoretical results show that $n_c = 9$ for VBO = 0.56 eV, whereas $n_c = 10$ for the other three VBO values. The last remark, but not the least important as regards figure 3, is that all of the theoretical curves meet in the region where $n \geqslant 10$ (the region of type-I SLs) independently of which VBO value is used. This clearly shows that band mixing is only effective when $n < n_c$ whereas the GaAs wells become completely separated when $n \geqslant n_c$ and thus the SL becomes of type I.

4. Conclusions

We have studied the electronic band structures of the (AlAs)$_m$(GaAs)$_n$(001) superlattices versus the layer thicknesses (m, n) and the valence band offset (VBO). The highest state in the SL valence band is found to be, always, confined to the GaAs slabs whereas the lowest state in the SL conduction band shows different behaviours as it is sensitive to the valley-mixing effects. Our tight-binding results favour a high valence band offset (VBO = 0.56 eV) and a small conduction band offset (CBO = 190 meV). These band offsets are necessitated by the ultrathin SLs exhibiting type-II behaviour. Providing that these offset values are achieved, for most of the ultrathin-layer SLs ($m, n \leqslant 8$), the strong band-mixing effects enhance the AlAs X$_{xy}$ valley to become the lowest in the CB and, as a result, the SL behaves as a type-II

structure with an indirect bandgap. In the rest of the ultrathin-layer SLs, whenever the GaAs slabs are thick enough, the electronic confinement energy becomes small in the GaAs wells and, therefore, the SL behaves as a type-I structure with a direct bandgap at the Γ point.

For thick-layer SLs ($m, n \geqslant 9$), there exists a critical barrier thickness beyond which the GaAs wells become completely decoupled and the SL behaves as a type-I structure with a direct bandgap at the Γ point. Our band-structure results for the $(AlAs)_n(GaAs)_n(001)$ SLs, when VBO = 0.56 eV, suggested a critical layer thickness ($n_c = 9$) of about 26 Å for the type-I–type-II transition. This n_c-value is consistent with the photoreflectance experiments [6].

Finally, thick-layer SLs ($m, n \geqslant 9$) are definitely more suitable for photonic applications as they behave as type-I SLs and possess direct-bandgap energies lying within the energy spectrum of visible light. These SLs do, indeed, exhibit very high radiative efficiency. On the other hand, the very recent results of photoluminescence experiments [8], which found that the ultrathin-layer SLs can also behave as type-I SLs at room temperature, have opened up a new area of investigation which we plan to address in future work.

Acknowledgments

References

[1] For a review see, for instance, Kelly M J and Nicholas R J 1985 *Rep. Prog. Phys.* **48** 1699
[2] Dawson P, Moore K J, Foxon C T, t'Hooft G W and van Hal R P M 1989 *J. Appl. Phys.* **65** 3606
[3] Scalbert D, Cernogora J, Benoît à la Guillaume C, Maaref M, Charfi F F and Planel R 1989 *Solid State Commun.* **70** 945
[4] Meynadier M H, Nahory R E, Worlock J M, Tamargo M C, de Miguel J L and Sturge M D 1988 *Phys. Rev. Lett.* **60** 1338
[5] Teissier R, Finley J J, Skolnick M S, Cockburn J W, Pelouard J L, Grey R, Hill G, Pate M A and Planel R 1996 *Phys. Rev.* B **54** R8329
[6] Fujimoto H, Hamaguchi C, Nakagawa T, Taniguchi K, Imanishi K, Kato H and Watanabe Y 1990 *Phys. Rev.* B **41** 7593
[7] Matsuoka T, Nakazawa T, Ohya T, Taniguchi K, Hamaguchi C, Kato H and Watanabe Y 1991 *Phys. Rev.* B **43** 11 798
[8] Schwabe R, Pietag F, Gottschalch V, Wagner G, Di Ventra M, Bitz A and Staehli J L 1997 *Phys. Rev.* B **56** R4329
[9] Zhang S B, Cohen M L and Louie S G 1991 *Phys. Rev.* B **43** 9951
[10] Ting D Z Y and Chang Y C 1987 *Phys. Rev.* B **36** 4359
[11] Schulman J N and McGill T C 1979 *Phys. Rev.* B **19** 6341
[12] Mon K K 1982 *Solid State Commun.* **41** 699
[13] Nara S 1987 *Japan. J. Appl. Phys.* **26** 690
    Nara S 1987 *Japan. J. Appl. Phys.* **26** 1713
[14] Yamaguchi E 1987 *J. Phys. Soc. Japan* **56** 2835
[15] Ihm J 1987 *Appl. Phys. Lett.* **50** 1068
[16] Muñoz M C, Velasco V R and Garcia-Moliner F 1989 *Phys. Rev.* B **39** 1786
[17] Lu Y T and Sham L J 1989 *Phys. Rev.* B **40** 5567
[18] Anderioni W and Car R 1980 *Phys. Rev.* B **21** 3334
[19] Nakayama T and Kamimura H 1985 *J. Phys. Soc. Japan* **54** 4726
[20] Gell M A, Ninno D, Jaros M and Herbert D C 1986 *Phys. Rev.* B **34** 2416
[21] Gell M A, Jaros M and Herbert D C 1997 *Superlatt. Microstruct.* **3** 121
[22] Xia Jian-Bai 1988 *Phys. Rev.* B **38** 8358
[23] Bylander D M and Kleinman L 1987 *Phys. Rev.* B **36** 3229
[24] Nelson J S, Fong C Y, Batra I P, Pickett W E and Klein B M 1988 *Phys. Rev.* B **37** 10 203
[25] Wei S H and Zunger A 1988 *J. Appl. Phys.* **63** 5794
[26] Cardona M, Suemota T, Christensen N E, Isu T and Ploog K 1987 *Phys. Rev.* B **36** 5906

[27] Eppenga R and Schuurmans M F H 1988 *Phys. Rev.* B **38** 3541
[28] Zhang S B, Hybertson M S, Cohen M L, Louie S G and Tomanek D 1989 *Phys. Rev. Lett.* **63** 1495
[29] Gordon R J, Ikonic Z and Srivastava G P 1990 *Semicond. Sci. Technol.* **5** 269
[30] van Kesteren H W, Cosman E C, Greidanus F, Dawson P, Moore K J and Foxon C T 1988 *Phys. Rev. Lett.* **61** 129
[31] Godby R W, Schlüter M and Sham L J 1988 *Phys. Rev.* B **37** 10 159
[32] Vogl P, Hjalmarson H P and Dow J D 1983 *J. Phys. Chem. Solids* **44** 365
[33] *Landolt–Börnstein New Series (Numerical Data and Functional Relationships in Science and Technology)* 1982 vol 17a, ed K H Hellwege and O Madelung (Berlin: Springer)
[34] Dingle R 1975 *Festkörperprobleme (Advances in Solid State Physics)* vol 15, ed H J Queisser (Braunschweig: Vieweg–Pergamon)
[35] Kroemer H 1986 *Proc. 12th Yamada Conf. on Modulated Semiconductor Structures; Surf. Sci.* **174** ed H Sakaki and see also reference [36].
[36] Miller R C, Kleinman D A and Gossard A C 1984 *Phys. Rev.* B **29** 7085
[37] Löwdin P O 1950 *J. Chem. Phys.* **18** 365
[38] Cullum J K and Willoughby R A 1985 *Theory (Lanczos Algorithm for Large Eigenvalue Computations vol 1)* (Basel: Birkhäuser)
[39] Tit N 1997 *J. Phys.: Condens. Matter* **9** 6505
[40] Batey J and Wright S L 1986 *J. Appl. Phys.* **59** 200
[41] Arnold D, Ketterson A, Henderson T, Klem J and Morkoc H 1985 *J. Appl. Phys.* **57** 2880
[42] Frensley W R and Kroemer H 1976 *J. Vac. Sci. Technol.* **13** 810
[43] Baldereschi A, Baroni S and Resta R 1988 *Phys. Rev. Lett.* **61** 734
[44] Van de Walle C 1989 *Phys. Rev.* B **39** 1871
[45] Ishibashi A, Mori Y, Itahashi M and Watanabe N 1985 *J. Appl. Phys.* **58** 2691
[46] Isu T, Jiang De-Sheng and Ploog K 1987 *Appl. Phys.* A **43** 75
[47] Finkman E, Sturge M D and Tamargo M C 1986 *Appl. Phys. Lett.* **49** 1299
[48] Moore K J, Dawson P and Foxon C T 1988 *Phys. Rev.* B **38** 3368
See also; Miller R C, Kleinman D A and Gossard A C 1984 *Phys. Rev.* B **29** 7085